

Convex Relaxations of Optimal Power Flow Problems: An Illustrative Example

Daniel K. Molzahn, *Member, IEEE*, and Ian A. Hiskens, *Fellow, IEEE*

Abstract—Recently, there has been significant interest in convex relaxations of the optimal power flow (OPF) problem. A semidefinite programming (SDP) relaxation globally solves many OPF problems. However, there exist practical problems for which the SDP relaxation fails to yield the global solution. Conditions for the success or failure of the SDP relaxation are valuable for determining whether the relaxation is appropriate for a given OPF problem. To move beyond existing conditions, which only apply to a limited class of problems, a typical conjecture is that failure of the SDP relaxation can be related to physical characteristics of the system. By presenting an example OPF problem with two equivalent formulations, this paper demonstrates that physically based conditions cannot universally explain algorithm behavior. The SDP relaxation fails for one formulation but succeeds in finding the global solution to the other formulation. Since these formulations represent the same system, success (or otherwise) of the SDP relaxation must involve factors beyond just the network physics. The lack of universal physical conditions for success of the SDP relaxation motivates the development of tighter convex relaxations capable of solving a broader class of problems. Tools from polynomial optimization theory provide a means of developing tighter relaxations. This paper uses the example problem to illustrate relaxations from the Lasserre hierarchy for polynomial optimization and a related “mixed semidefinite/second-order cone programming” hierarchy.

Index Terms—Convex relaxation, global solution, optimal power flow, power system optimization.

I. INTRODUCTION

THE optimal power flow (OPF) problem determines a minimum cost operating point for an electric power system subject to both network constraints and engineering limits. Typical objectives are minimization of losses or generation costs. The OPF problem is generally non-convex due to the non-linear power flow equations [1] and may have local solutions [2]. OPF solution techniques are therefore an ongoing research topic. Many techniques have been proposed, including successive quadratic programs, Lagrangian relaxation, and interior point methods [3]–[7].

Manuscript received October 5, 2015; revised January 9, 2016; accepted February 3, 2016. Date of publication June 7, 2016; date of current version June 28, 2016. This work was supported by the Dow Sustainability Fellowship, ARPA-E under Grant DE-AR0000232, and Los Alamos National Laboratory under Subcontract 270958. This paper was recommended by Associate Editor M. di Bernardo.

The authors are with the Department of Electrical Engineering and Computer Science, University of Michigan, Ann Arbor, MI 48109-2121 USA (e-mail: molzahn@umich.edu; hiskens@umich.edu).

Color versions of one or more of the figures in this paper are available online at <http://ieeexplore.ieee.org>.

Digital Object Identifier 10.1109/TCSI.2016.2529281

There has been significant interest in convex relaxations of OPF problems. Convex relaxations lower bound the objective value, can certify infeasibility, and, in many cases, globally solve OPF problems. In contrast, traditional OPF solution methods may find the global optimum [8] but provide no guarantee of doing so, do not provide a measure of solution quality and cannot provably identify infeasibility. The capabilities of convex relaxations thus supplement traditional techniques.

For radial systems that satisfy certain non-trivial technical conditions [9], a second-order cone programming (SOCP) relaxation is provably *exact* (i.e., the lower bound is tight and the solution provides the globally optimal decision variables). For more general OPF problems, a semidefinite programming (SDP) based Shor relaxation [10] is often exact [11], [12]. Active research in this area includes developing tighter and faster relaxations with improved modeling flexibility as well as distributed solution algorithms [13]–[25].

Despite success in globally solving many practical OPF problems [12], [13], there are problems for which the SDP relaxation of [12] is not exact [2], [13], [26], [27]. There is substantial interest in developing sufficient conditions for exactness of the SDP relaxation. Existing conditions include requirements on power injection, voltage magnitude, and line-flow limits, and either radial networks (typical of distribution systems), appropriate placement of controllable phase-shifting transformers, or a limited subset of mesh network topologies [9], [28].

The SDP relaxation globally solves many OPF problems which do not satisfy any known sufficient conditions [9], [28]. In other words, the set of problems guaranteed to be exact by known conditions is much smaller than the actual set of problems for which the relaxation is exact. This suggests the potential for developing less stringent conditions. It is natural to speculate that some physical characteristics of an OPF problem may govern such conditions. With solutions close to voltage collapse, this speculation is supported by several problems for which the SDP relaxation is not exact [27].

This paper’s first contribution is an example that dampens enthusiasm for this avenue of research. We consider a small problem, first presented in [29], with two equivalent formulations. The SDP relaxation globally solves one formulation but fails to solve the other. Since both formulations represent the same system, strictly physically based conditions for the success of the relaxation cannot differentiate between these formulations.¹ The feasible spaces of both problems illustrate

¹See also [28] for an example where different line-flow limit formulations determine success or failure of the SDP relaxation.

why the SDP relaxation succeeds for one formulation but fails for the other.

The small example considered in this paper is relatively simple. In fact, this example ‘‘OPF’’ problem reduces to finding the minimum loss solution to power flow constraint equations for a specified set of power injections and voltage magnitudes. Thus, this example further demonstrates that the SDP relaxation may fail even for simple OPF problems.

The lack of universal, physically based conditions for determining success or failure of the SDP relaxation of [12] motivates the development of tighter convex relaxations. Recent research [30]–[34] exploits the fact that the OPF problem is a polynomial optimization problem in terms of the complex voltage phasors. Separating the complex voltages into real and imaginary parts yields a polynomial optimization problem in real variables. This facilitates the application of the Lasserre hierarchy of ‘‘moment’’ relaxations for real polynomial optimization problems, which take the form of SDPs [35]. The first-order moment relaxation is equivalent to the SDP relaxation of [12]. Higher-order moment relaxations thus generalize the SDP relaxation of [12], enabling global solution of many problems for which the SDP relaxation of [12] is not exact [30]–[34].

The ability of the moment relaxations to solve a broader class of OPF problems comes at a computational cost: the matrices grow rapidly with both relaxation order and system size. Ameliorating the former challenge, low relaxation orders suffice for global solution of many problems. Several recent developments address the latter challenge. First, by exploiting sparsity and selectively applying the higher-order constraints to specific buses, loss-minimization problems with thousands of buses are computationally tractable [33], [34]. Second, rather than separating complex voltages into their real and imaginary parts, a hierarchy built directly from the complex formulation is computationally advantageous [36]. Third, emerging SDP solution algorithms may enable faster computation of the moment relaxations [21], [37], [38]. Fourth, a ‘‘mixed SDP/SOCP’’ hierarchy implements the first-order constraints with an SDP formulation, but the higher-order constraints are relaxed to an SOCP formulation [39]. The less computationally intensive SOCP constraints often reduce solution times while still yielding global optima.

The second contribution of this paper is a tutorial-style review of the moment relaxation and mixed SDP/SOCP hierarchies in the context of the small example system. By illustrating the corresponding feasible spaces, the small example system is used to demonstrate the varying capabilities of the relaxations to globally solve OPF problems. Further, presentation of the matrices and related discussion for the small example system clarify implementation details regarding the various relaxation hierarchies.

This paper is organized as follows. Section II introduces the OPF problem. Section III describes the SDP relaxation of [12]. Section IV presents the example OPF problem which demonstrates that factors beyond the problem physics determine success or failure of the SDP relaxation. Sections V and VI provide the moment relaxations using SDP constraints and the mixed SDP/SOCP hierarchy, respectively, with the problem

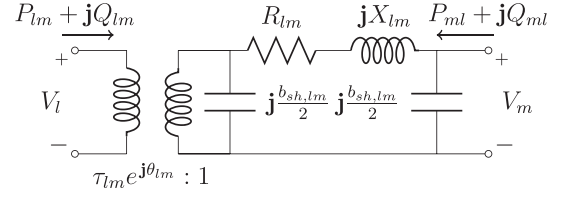


Fig. 1. Line model.

in Section IV providing an illustrative example. Section VII concludes the paper.

II. OPTIMAL POWER FLOW PROBLEM

We first present an OPF formulation in terms of rectangular voltage coordinates, active and reactive power injections, and apparent power line flow limits. Consider an n -bus system with n_l lines, where $\mathcal{N} = \{1, \dots, n\}$ is the set of buses, \mathcal{G} is the set of generator buses, and \mathcal{L} is the set of lines. The network admittance matrix is $\mathbf{Y} = \mathbf{G} + \mathbf{jB}$, where \mathbf{j} denotes the imaginary unit. Let $P_{Dk} + \mathbf{j}Q_{Dk}$ represent the active and reactive load demand and $V_k = V_{dk} + \mathbf{j}V_{qk}$ the voltage phasors at each bus $k \in \mathcal{N}$. Superscripts ‘‘max’’ and ‘‘min’’ denote specified upper and lower limits. Buses without generators have maximum and minimum generation set to zero.

Define a function for squared voltage magnitude:

$$f_{V_k}(V_d, V_q) := V_{dk}^2 + V_{qk}^2. \quad (1)$$

The power flow equations describe the network physics:

$$\begin{aligned} f_{P_k}(V_d, V_q) := & V_{dk} \sum_{i=1}^n (\mathbf{G}_{ki} V_{di} - \mathbf{B}_{ki} V_{qi}) \\ & + V_{qk} \sum_{i=1}^n (\mathbf{B}_{ki} V_{di} + \mathbf{G}_{ki} V_{qi}) + P_{Dk} \end{aligned} \quad (2a)$$

$$\begin{aligned} f_{Q_k}(V_d, V_q) := & V_{dk} \sum_{i=1}^n (-\mathbf{B}_{ki} V_{di} - \mathbf{G}_{ki} V_{qi}) \\ & + V_{qk} \sum_{i=1}^n (\mathbf{G}_{ki} V_{di} - \mathbf{B}_{ki} V_{qi}) + Q_{Dk}. \end{aligned} \quad (2b)$$

Define a convex quadratic cost of active power generation:

$$f_{C_k}(V_d, V_q) := c_{k2} (f_{P_k}(V_d, V_q))^2 + c_{k1} f_{P_k}(V_d, V_q) + c_{k0}. \quad (3)$$

We use a line model with an ideal transformer that has a specified turns ratio $\tau_{lm} e^{j\theta_{lm}} : 1$ in series with a Π circuit with series impedance $R_{lm} + \mathbf{j}X_{lm}$ (equivalent to an admittance of $g_{lm} + \mathbf{j}b_{lm} := 1/(R_{lm} + \mathbf{j}X_{lm})$) and total shunt susceptance $\mathbf{j}b_{sh,lm}$. (See Fig. 1.) The line flow equations are:

$$\begin{aligned} f_{P_{lm}}(V_d, V_q) := & \frac{(V_{dl}^2 + V_{ql}^2) g_{lm}}{\tau_{lm}^2} + (V_{dl} V_{dm} + V_{ql} V_{qm}) \\ & \times (b_{lm} \sin(\theta_{lm}) - g_{lm} \cos(\theta_{lm})) / \tau_{lm} \\ & + (V_{dl} V_{qm} - V_{ql} V_{dm}) \\ & \times (g_{lm} \sin(\theta_{lm}) + b_{lm} \cos(\theta_{lm})) / \tau_{lm} \end{aligned} \quad (4a)$$

$$\begin{aligned}
f_{Qlm}(V_d, V_q) &:= -(V_{dl}^2 + V_{ql}^2) \left(b_{lm} + \frac{b_{sh,lm}}{2} \right) / \tau_{lm}^2 \\
&+ (V_{dl}V_{dm} + V_{ql}V_{qm}) \\
&\times (b_{lm} \cos(\theta_{lm}) + g_{lm} \sin(\theta_{lm})) / \tau_{lm} \\
&+ (V_{dl}V_{qm} - V_{ql}V_{dm}) \\
&\times (g_{lm} \cos(\theta_{lm}) - b_{lm} \sin(\theta_{lm})) / \tau_{lm}
\end{aligned} \tag{4b}$$

$$f_{Slm}(V_d, V_q) := (f_{Plm}(V_d, V_q))^2 + (f_{Qlm}(V_d, V_q))^2 \tag{4c}$$

$$\begin{aligned}
f_{Pml}(V_d, V_q) &:= (V_{dm}^2 + V_{qm}^2) g_{lm} - (V_{dl}V_{dm} + V_{ql}V_{qm}) \\
&\times (g_{lm} \cos(\theta_{lm}) + b_{lm} \sin(\theta_{lm})) / \tau_{lm} \\
&+ (V_{dl}V_{qm} - V_{ql}V_{dm}) \\
&\times (g_{lm} \sin(\theta_{lm}) - b_{lm} \cos(\theta_{lm})) / \tau_{lm}
\end{aligned} \tag{4d}$$

$$\begin{aligned}
f_{Qml}(V_d, V_q) &:= -(V_{dm}^2 + V_{qm}^2) \left(b_{lm} + \frac{b_{sh,lm}}{2} \right) \\
&+ (V_{dl}V_{dm} + V_{ql}V_{qm}) \\
&\times (b_{lm} \cos(\theta_{lm}) - g_{lm} \sin(\theta_{lm})) / \tau_{lm} \\
&+ (-V_{dl}V_{qm} + V_{ql}V_{dm}) \\
&\times (g_{lm} \cos(\theta_{lm}) + b_{lm} \sin(\theta_{lm})) / \tau_{lm}
\end{aligned} \tag{4e}$$

$$f_{Sml}(V_d, V_q) := (f_{Pml}(V_d, V_q))^2 + (f_{Qml}(V_d, V_q))^2. \tag{4f}$$

The OPF problem is:

$$\min_{V_d, V_q} \sum_{k \in \mathcal{G}} f_{Ck}(V_d, V_q) \quad \text{subject to} \tag{5a}$$

$$P_{Gk}^{\min} \leq f_{Pk}(V_d, V_q) \leq P_{Gk}^{\max} \quad \forall k \in \mathcal{N} \tag{5b}$$

$$Q_{Gk}^{\min} \leq f_{Qk}(V_d, V_q) \leq Q_{Gk}^{\max} \quad \forall k \in \mathcal{N} \tag{5c}$$

$$(V_k^{\min})^2 \leq f_{Vk}(V_d, V_q) \leq (V_k^{\max})^2 \quad \forall k \in \mathcal{N} \tag{5d}$$

$$f_{Slm}(V_d, V_q) \leq (S_{lm}^{\max})^2 \quad \forall (l, m) \in \mathcal{L} \tag{5e}$$

$$f_{Sml}(V_d, V_q) \leq (S_{lm}^{\max})^2 \quad \forall (l, m) \in \mathcal{L} \tag{5f}$$

$$V_{q1} = 0. \tag{5g}$$

Constraint (5g) sets the reference bus angle to zero.

III. SEMIDEFINITE RELAXATION OF THE OPF PROBLEM

This section describes an SDP relaxation of the OPF problem adopted from [12], [13], [15]. We use notation from [30], [33] corresponding to the moment relaxations that will be introduced in the following sections. We begin with several definitions. Define the vector of real decision variables $\hat{x} \in \mathbb{R}^{2n}$ as

$$\hat{x} := [V_{d1} \quad V_{d2} \quad \dots \quad V_{qn}]^\top \tag{6}$$

where $(\cdot)^\top$ denotes the transpose.² A monomial is defined using a vector $\alpha \in \mathbb{N}^{2n}$ of exponents: $\hat{x}^\alpha := V_{d1}^{\alpha_1} V_{d2}^{\alpha_2} \dots V_{qn}^{\alpha_{2n}}$. A polynomial is $g(\hat{x}) := \sum_{\alpha \in \mathbb{N}^{2n}} g_\alpha \hat{x}^\alpha$, where g_α is the real scalar coefficient corresponding to the monomial \hat{x}^α .

Define a linear functional $L_y\{g\}$ which replaces the monomials \hat{x}^α in a polynomial $g(\hat{x})$ with real scalar variables y :

$$L_y\{g\} := \sum_{\alpha \in \mathbb{N}^{2n}} g_\alpha y_\alpha. \tag{7}$$

For a matrix $g(\hat{x})$, $L_y\{g\}$ is applied componentwise to each element of $g(\hat{x})$.

Consider, for example, the vector $\hat{x} = [V_{d1} \quad V_{d2} \quad V_{q2}]^\top$ corresponding to the voltage components of a two-bus system, where the angle reference (5g) is used to eliminate V_{q1} . Consider also the polynomial $g(\hat{x}) = (V_2^{\max})^2 - V_{d2}^2 - V_{q2}^2$. (The constraint $g(\hat{x}) \geq 0$ forces the voltage magnitude at bus 2 to be less than or equal to V_2^{\max} .) Then $L_y\{g\} = (V_2^{\max})^2 y_{000} - y_{020} - y_{002}$. Thus, $L_y\{g\}$ converts a polynomial $g(\hat{x})$ to a linear function of y .

The convex quadratic cost functions (3) for each generator $k \in \mathcal{G}$ are implemented by minimizing an auxiliary variable ω_k constrained by the SOCP formulation in (8e) [15].

The SDP relaxation of (5) is:

$$\min_{y, \omega} \sum_{k \in \mathcal{G}} \omega_k \quad \text{subject to} \tag{8a}$$

$$P_{Gk}^{\min} \leq L_y\{f_{Pk}\} \leq P_{Gk}^{\max} \quad \forall k \in \mathcal{N} \tag{8b}$$

$$Q_{Gk}^{\min} \leq L_y\{f_{Qk}\} \leq Q_{Gk}^{\max} \quad \forall k \in \mathcal{N} \tag{8c}$$

$$(V_k^{\min})^2 \leq L_y\{f_{Vk}\} \leq (V_k^{\max})^2 \quad \forall k \in \mathcal{N} \tag{8d}$$

$$\begin{aligned}
&(1 - c_{k1} L_y\{f_{Pk}\} - c_{k0} + \omega_k) \\
&\geq \left\| \begin{bmatrix} (1 + c_{k1} L_y\{f_{Pk}\} + c_{k0} - \omega_k) \\ 2\sqrt{c_{k2}} L_y\{f_{Pk}\} \end{bmatrix} \right\|_2 \quad \forall k \in \mathcal{G}
\end{aligned} \tag{8e}$$

$$S_{lm}^{\max} \geq \left\| \begin{bmatrix} L_y\{f_{Plm}\} \\ L_y\{f_{Qlm}\} \end{bmatrix} \right\|_2 \quad \forall (l, m) \in \mathcal{L} \tag{8f}$$

$$S_{lm}^{\max} \geq \left\| \begin{bmatrix} L_y\{f_{Pml}\} \\ L_y\{f_{Qml}\} \end{bmatrix} \right\|_2 \quad \forall (l, m) \in \mathcal{L} \tag{8g}$$

$$L_y\{\hat{x}\hat{x}^\top\} \succeq 0 \tag{8h}$$

$$y_{00\dots 0} = 1 \tag{8i}$$

$$y_{**\dots\rho*\dots} = 0 \quad \rho = 1, 2, \tag{8j}$$

where $\succeq 0$ indicates positive semidefiniteness of the corresponding matrix and $\|\cdot\|_2$ denotes the two-norm. The apparent power flow constraints (5e) and (5f) are implemented with the SOCP formulations in (8f) and (8g). See [13] for a more general formulation of the SDP relaxation that considers the possibilities of multiple generators per bus and convex

²The ability to arbitrarily set an angle reference in the OPF problem enables the choice of one arbitrarily selected variable. We choose $V_{q1} = 0$ as in (5g).

piecewise-linear generation costs. The constraint (8i) enforces the fact that $\hat{x}^0 = 1$. The constraint (8j) corresponds to the angle reference $V_{q1} = 0$; the ρ in (8j) is in the index $n + 1$, which corresponds to the variable V_{q1} . Note that the angle reference can alternatively be used to eliminate all terms corresponding to V_{q1} to reduce the size of the semidefinite program.

If the condition $\text{rank}(L_y\{\hat{x}\hat{x}^\top\}) = 1$ is satisfied, the relaxation is “exact” and the global solution to (5) is recovered using an eigen-decomposition. Consider a solution to (8) where the rank of the matrix $L_y\{\hat{x}\hat{x}^\top\}$ is equal to one with non-zero eigenvalue λ and associated unit-length eigenvector η . The globally optimal voltage phasor solution to (5) is

$$V^* = \sqrt{\lambda} (\eta_{1:n} + \mathbf{j}\eta_{(n+1):2n}) \quad (9)$$

where subscripts denote vector entries in MATLAB notation.

The computational bottleneck of the SDP relaxation is the constraint (8h), which enforces positive semidefiniteness of a $2n \times 2n$ matrix. Solving the SDP relaxation of large OPF problems requires exploiting network sparsity. A matrix completion decomposition exploits sparsity by converting the positive semidefinite constraint on the large matrix in (8h) to positive semidefinite constraints on many smaller submatrices. These submatrices are defined using the cliques (i.e., completely connected subgraphs) of a chordal extension of the power system network graph. See [13], [15], [40] for a full description of a formulation that enables solution of (8) for systems with thousands of buses.

IV. EQUIVALENT FORMULATIONS OF A SMALL EXAMPLE PROBLEM

The SDP relaxation (8) globally solves many OPF problems which do not satisfy any known sufficient conditions guaranteeing exactness [9], [28], indicating the potential for development of broader sufficient conditions. One speculation is that some physical characteristic of the OPF problem predicts the relaxation’s success or failure.

The following example shows that strictly physically based sufficient conditions are unable to definitively predict success or failure of the SDP relaxation for all OPF problems. The example problem has equivalent two- and three-bus formulations. The relaxation globally solves the two-bus system. For the three-bus system, however, the relaxation only gives a strict lower bound on the objective value rather than the solution.

A. Example Problem

Consider the two- and three-bus systems in Figs. 2 and 3. For both systems, the voltage magnitudes at buses 1 and 2 are fixed to 1.0 and 1.3 per unit, respectively, and the active power injection at bus 2 is fixed to zero.³ There are no limits on the reactive power injections at buses 1 and 2. For bus 3 in the three-bus system, the active and reactive power injections are constrained to zero and there is no voltage magnitude constraint. With the active power injections at the other buses fixed

³Equality constraints are achieved by setting the upper and lower limits equal (e.g., $V_1^{\max} = V_1^{\min} = 1$ per unit).

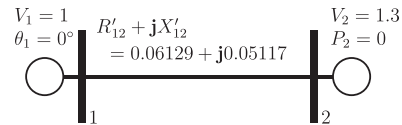


Fig. 2. Two-bus system.

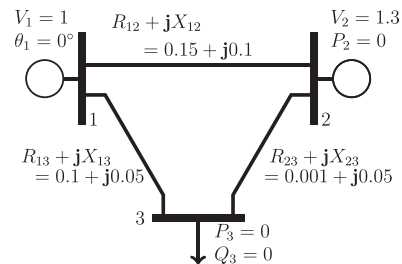


Fig. 3. Three-bus system.

TABLE I
SOLUTIONS TO TWO- AND THREE-BUS SYSTEMS (PER UNIT)

	Two-Bus System	Three-Bus System
$V_{d1} + \mathbf{j}V_{q1}$	1.000 + $\mathbf{j}0.000$	1.000 + $\mathbf{j}0.000$
$V_{d2} + \mathbf{j}V_{q2}$	1.049 - $\mathbf{j}0.767$	1.049 - $\mathbf{j}0.767$
$V_{d3} + \mathbf{j}V_{q3}$	N/A	0.849 - $\mathbf{j}0.586$
$P_1 + \mathbf{j}Q_1$	5.68 - $\mathbf{j}7.77$	5.68 - $\mathbf{j}7.77$
$P_2 + \mathbf{j}Q_2$	0.0 + $\mathbf{j}12.52$	0.0 + $\mathbf{j}12.52$
$P_3 + \mathbf{j}Q_3$	N/A	0.0 + $\mathbf{j}0$

to zero, the objective function minimizes active power injection at bus 1.

The resistance-to-reactance ratios for lines in both the two- and three-bus systems are somewhat atypical for transmission systems, but are not particularly unusual for more lossy networks like subtransmission and distribution systems [41]. Similar characteristics to these systems may also occur when using “equivalencing” techniques to reduce larger systems to a smaller representative network [42], [43].

With two quantities specified at each bus k along with two degrees of freedom (V_{dk} and V_{qk}), the feasible space for the OPF problem (5) for this example consists of a set of isolated points that are the solutions of the power flow equations. The OPF finds the solution point that has the lowest active power losses. Here, this solution corresponds to the “high-voltage/small angle-difference” power flow solution, which is commonly calculated using a Newton-Raphson iteration initialized from a flat start (i.e., voltages of $1\angle 0^\circ$).⁴ In this paper, however, we use this problem to explore the properties of the convex relaxations.

Since bus 3 in the three-bus system has zero power injections, it can be eliminated by adding $R_{13} + \mathbf{j}X_{13}$ and $R_{23} + \mathbf{j}X_{23}$ to yield an equivalent two-bus system with two parallel lines.⁵ The

⁴For both two- and three-bus systems, (5) has one other local minimum: there exists one “low-voltage/large angle-difference” power flow solution with larger losses.

⁵Elimination of bus 3 requires that the zero power injection at this bus is achieved using an “open circuit to ground.” A “short circuit to ground” could also yield zero power injections. However, a short circuit at bus 3 results in infeasibility of the power flow equations for the loading specified in Fig. 3. Thus, the feasible space of the two-bus system in Fig. 2 can be directly mapped to the feasible space of the three-bus system in Fig. 3.

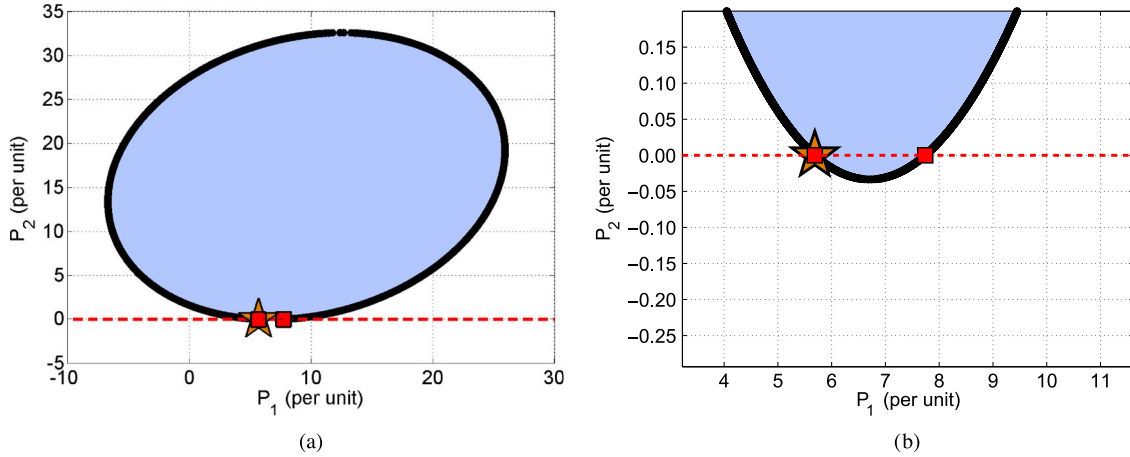


Fig. 4. Projection of the two-bus system’s feasible space. The red squares at the intersection of the black oval and red dashed line are the feasible space for the OPF problem (5). The blue region, including the black oval boundary, is the feasible space for the SDP relaxation (8). The orange star is the solution to the SDP relaxation, which is the global optimum for the two-bus system. (a) Projection of the two-bus system’s feasible space. (b) Zoomed view of (a).

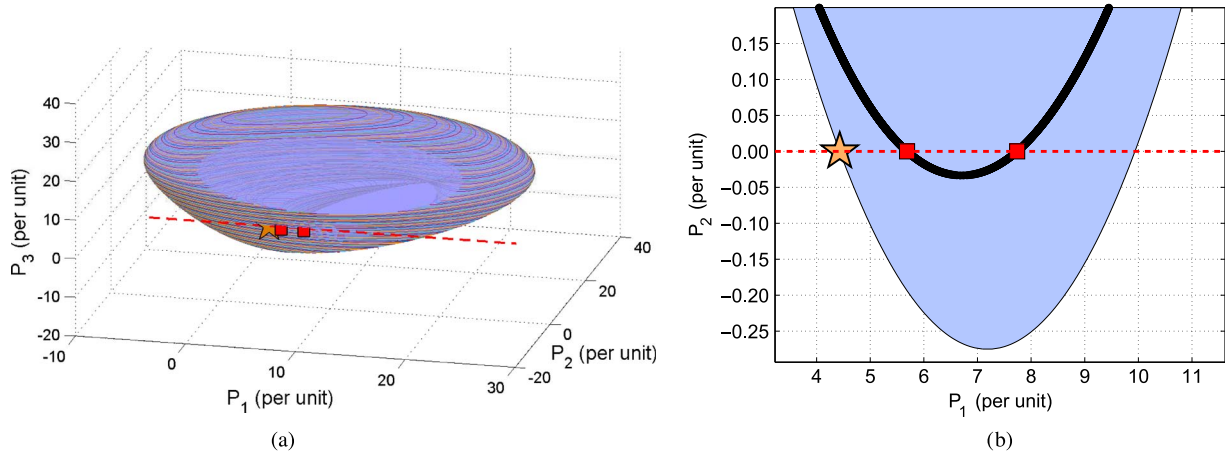


Fig. 5. Projection of the three-bus system’s feasible space. The feasible space for the OPF problem (5) is denoted by the red squares at the intersection of the red dashed line and the region formed by the colored lines in (a) (the black line in (b)). The blue region is the feasible space for the SDP relaxation (8). The orange star is the solution to the SDP relaxation, which does not match the global solution at the leftmost red square. (a) Projection of the three-bus system’s feasible space. (b) Projection of the three-bus system’s feasible space with $P_3 = 0$.

parallel combination of these lines gives the line impedance $R'_{12} + jX'_{12}$ shown in the two-bus system of Fig. 2. Thus, the OPF problems for the two- and three-bus systems are *equivalent*. The voltage at bus 3 in the three-bus system can be directly computed from the solution to the two-bus system. The global solutions are given in Table I.

The SDP relaxation globally solves the two-bus system. However, for the three-bus system, the relaxation only provides a lower bound that is 22% less than the true global optimum (i.e., there exists a large relaxation gap). We note that MATPOWER’s interior point solver [7] fails to converge for the three-bus formulation of this problem but successfully solves the two-bus formulation.

B. Feasible Space Exploration

Although the OPF problems (5) for the two- and three-bus systems share the same feasible spaces, this is not the case for their SDP relaxations (8). This section explores the feasible

spaces of these relaxations to illustrate why the SDP relaxation globally solves the two-bus system but fails for the equivalent three-bus system.

Figs. 4 and 5 show projections of the feasible spaces of the two- and three-bus systems in terms of the active power injections. The boundary of the oval, shown by the black line in Fig. 4, is the feasible space of the OPF problem (5) for varying values of P_2 . The region in Fig. 4 consisting of the oval and its interior is the feasible space of the SDP relaxation. For the specified value of $P_2 = 0$, shown by the red dashed line, the OPF problem has a feasible space consisting of the two red squares at the intersection of the red dashed line and the black oval. The SDP relaxation finds the global optimum of (5) (i.e., the leftmost red square) at the orange star.

In Fig. 5(a), the colored lines outline the feasible space of the OPF problem (5) for varying values of P_2 and P_3 , as determined using the approach in [44] and validated using repeated homotopy calculations [45]. This feasible space has an ellipsoidal shape with a hole in the interior. The red dashed line

corresponds to zero active power injections at buses 2 and 3. The OPF solutions, which are shown by the red squares at the intersection of the exterior of the ellipsoidal shape with the red dashed line, are near the hole in the feasible space. The feasible space of the SDP relaxation, shown by the shaded region, “stretches over” this hole in the OPF’s feasible space. As seen in Fig. 5(b), which shows a zoomed view of a cut through $P_3 = 0$, the exterior of the relaxation’s feasible space does not match the feasible space of the OPF problem near this hole. Thus, the solution to the SDP relaxation (8) at the orange star does not match the global solution to the OPF problem (5) at the leftmost red square, and the SDP relaxation is not exact for this formulation. Similar phenomena occur for a range of non-zero active power injections at bus 2.

The hole in the OPF’s feasible space is a non-convexity introduced by “nearby” problems (i.e., different values of P_3) in the three-bus system. Without the additional degrees of freedom associated with bus 3, there is no “nearby” non-convexity for the two-bus system. Thus, despite the fact that the OPF problems share the same feasible space (i.e., the red squares in Figs. 4 and 5), the SDP relaxation is exact for the two-bus system but not for the three-bus system.

V. MOMENT RELAXATIONS

By demonstrating that factors other than just physical characteristics determine success or failure of the SDP relaxation, the example in Section IV motivates the development of tighter convex relaxations that globally solve a broader class of OPF problems. Recognizing that the objective function and all constraints in the OPF problem are polynomial functions of the voltage phasor components enables the application of a hierarchy of convex “moment” relaxations from the Lasserre hierarchy for polynomial optimization problems. The moment relaxations, which converge to the global optimum of (5) with increasing relaxation order [35], generalize the SDP relaxation presented in Section III. This section introduces and illustrates the moment relaxations using the example from Section IV.

The moment relaxations require definitions beyond those in Section III. Define a vector x_γ consisting of all monomials of the voltage components V_d and V_q up to order γ :

$$x_\gamma := \begin{bmatrix} 1 & V_{d1} & \dots & V_{qn} & V_{d1}^2 & V_{d1}V_{d2} & \dots & V_{qn}^2 & V_{d1}^3 & V_{d1}^2V_{d2} & \dots & V_{qn}^\gamma \end{bmatrix}^\top. \quad (10)$$

The moment relaxations are composed of positive semi-definite constraints on *moment* and *localizing* matrices. The symmetric moment matrix \mathbf{M}_γ is composed of entries y_α corresponding to all monomials \hat{x}^α up to order 2γ :

$$\mathbf{M}_\gamma\{y\} := L_y\{x_\gamma x_\gamma^\top\}. \quad (11)$$

Symmetric localizing matrices are defined for each constraint of (5). For a polynomial constraint $g(\hat{x}) \geq 0$ of degree 2η , the localizing matrix is:

$$\mathbf{M}_{\gamma-\eta}\{gy\} := L_y\{gx_\gamma x_\gamma^\top\}. \quad (12)$$

See (14a)–(14c), at the bottom of the page, for the vector x_2 , moment matrix $\mathbf{M}_2\{y\}$, and the localizing matrix associated with upper voltage magnitude limit $(V_2^{\max})^2 - V_{d2}^2 - V_{q2}^2 \geq 0$, respectively, for a three-bus OPF problem. Note that the angle reference $V_{q1} = 0$ is used to eliminate V_{q1} in (14). These equations use the notation $L_y\{V_{d1}^{\alpha_1} V_{d2}^{\alpha_2} V_{d3}^{\alpha_3} V_{q2}^{\alpha_4} V_{q3}^{\alpha_5}\} = y_{\alpha_4 \alpha_5}^{\alpha_1 \alpha_2 \alpha_3}$.

The order- γ moment relaxation is:

$$\min_{y, \omega} \sum_{k \in \mathcal{G}} \omega_k \quad \text{subject to} \quad (13a)$$

$$\mathbf{M}_{\gamma-1}\{(f_{Pk} - P_k^{\min})y\} \succeq 0 \quad \forall k \in \mathcal{N} \quad (13b)$$

$$\mathbf{M}_{\gamma-1}\{(P_k^{\max} - f_{Pk})y\} \succeq 0 \quad \forall k \in \mathcal{N} \quad (13c)$$

$$\mathbf{M}_{\gamma-1}\{(f_{Qk} - Q_k^{\min})y\} \succeq 0 \quad \forall k \in \mathcal{N} \quad (13d)$$

$$\mathbf{M}_{\gamma-1}\{(Q_k^{\max} - f_{Qk})y\} \succeq 0 \quad \forall k \in \mathcal{N} \quad (13e)$$

$$\mathbf{M}_{\gamma-1}\{(f_{V_k} - (V_k^{\min})^2)y\} \succeq 0 \quad \forall k \in \mathcal{N} \quad (13f)$$

$$\mathbf{M}_{\gamma-1}\{(V_k^{\max})^2 - f_{V_k}\}y \succeq 0 \quad \forall k \in \mathcal{N} \quad (13g)$$

$$\begin{aligned} & (1 - c_{k1}L_y\{f_{Pk}\} - c_{k0} + \omega_k) \\ & \geq \left\| \begin{bmatrix} (1 + c_{k1}L_y\{f_{Pk}\} + c_{k0} - \omega_k) \\ 2\sqrt{c_{k2}}L_y\{f_{Pk}\} \end{bmatrix} \right\|_2 \quad \forall k \in \mathcal{G} \end{aligned} \quad (13h)$$

$$L_y\{f_{Ck}\} = \omega_k \quad \forall k \in \mathcal{G} \quad (13i)$$

$$\mathbf{M}_{\gamma-2}\{(S_{lm}^{\max})^2 - f_{Slm}\}y \succeq 0 \quad \forall (l, m) \in \mathcal{L} \quad (13j)$$

$$\mathbf{M}_{\gamma-2}\{(S_{ml}^{\max})^2 - f_{Sml}\}y \succeq 0 \quad \forall (l, m) \in \mathcal{L} \quad (13k)$$

$$S_{lm}^{\max} \geq \left\| \begin{bmatrix} L_y\{f_{Plm}\} \\ L_y\{f_{Qlm}\} \end{bmatrix} \right\|_2 \quad \forall (l, m) \in \mathcal{L} \quad (13l)$$

$$S_{lm}^{\max} \geq \left\| \begin{bmatrix} L_y\{f_{Pml}\} \\ L_y\{f_{Qml}\} \end{bmatrix} \right\|_2 \quad \forall (l, m) \in \mathcal{L} \quad (13m)$$

$$\mathbf{M}_\gamma\{y\} \succeq 0 \quad (13n)$$

$$y_{00\dots 0} = 1 \quad (13o)$$

$$y_{\star\dots\star\rho\star\dots\star} = 0 \quad \rho = 1, \dots, 2\gamma. \quad (13p)$$

where ρ in the angle reference constraint (13p) is in the index $n + 1$, which corresponds to the variable V_{q1} . In the same way as (8), the angle reference can alternatively be used to eliminate all terms corresponding to V_{q1} .⁶

As for the SDP relaxation, the globally optimal voltage phasors can be extracted using (9) from a solution to (13) that satisfies the condition $\text{rank}(L_y\{\hat{x}\hat{x}^\top\}) = 1$.

The order γ of the moment relaxation (13) must be greater than or equal to half of the degree of any polynomial in the OPF problem (5). This suggests that $\gamma \geq 2$ due to the fourth-order polynomials resulting from the objective function (5a) and the apparent power line flow constraints (5e) and (5f). However,

⁶We note that the angle reference constraint is unnecessary (i.e., its inclusion does not tighten the constraints) in the SDP relaxation [12] and the first-order moment relaxation [36]. However, the angle reference constraint (implemented either via eliminating V_{q1} or explicitly enforcing (13p)) can tighten the higher-order moment relaxations. For instance, the second-order moment relaxation with the angle reference constraint yields the globally optimal objective value of \$456.55 for the two-bus system in [46], but only a lower bound of \$452.61 without the angle reference constraint. (This phenomenon was not observed for the test case in Section IV.)

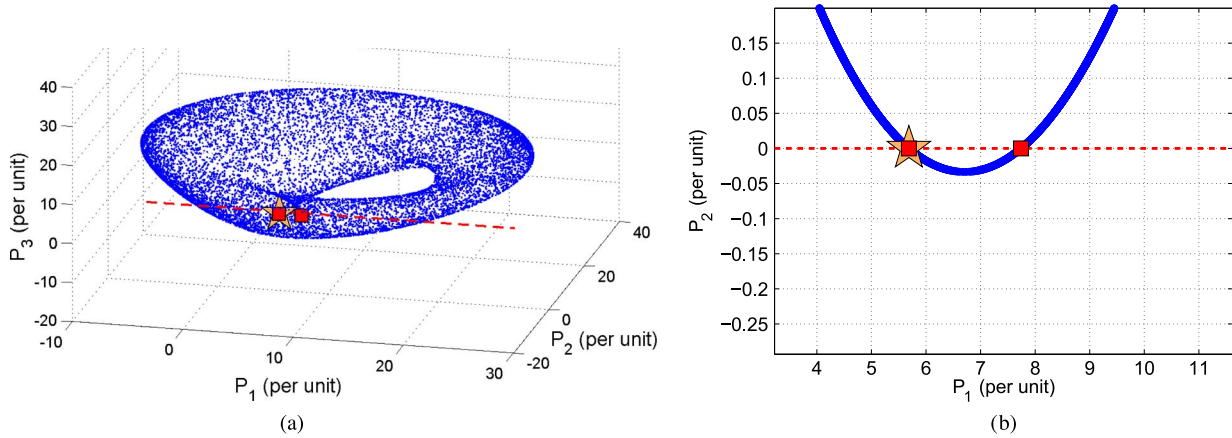


Fig. 6. Projection of the second-order moment relaxation’s feasible space for the three-bus system. The feasible space for the OPF problem (5) is denoted by the red squares. The second-order moment relaxation gives the global optimum at the orange star. The second-order moment relaxation was exact for all scenarios tested. (a) Projection of the second-order moment relaxation’s feasible space. (b) Projection of the feasible space shown in (a) with $P_3 = 0$.

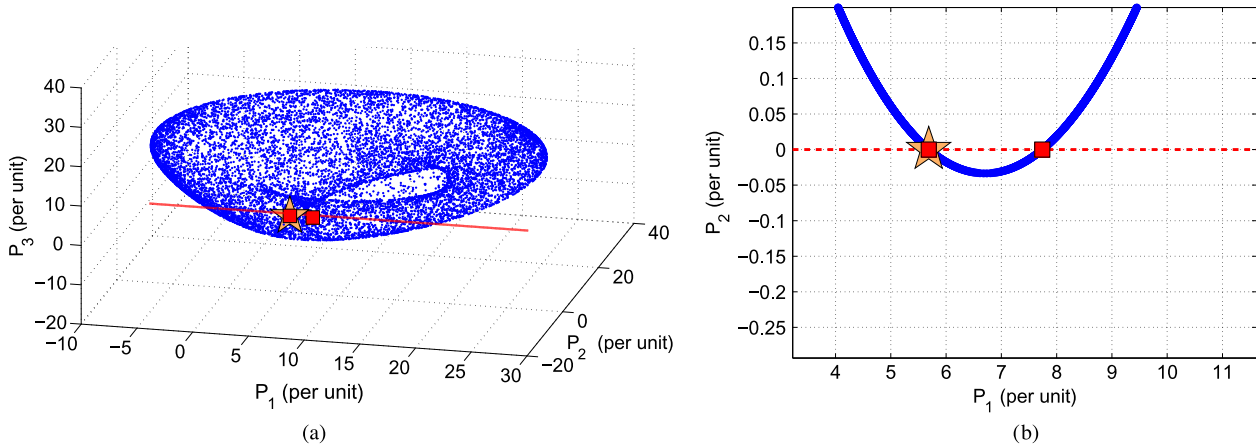


Fig. 7. Projection of the second-order mixed SDP/SOCP relaxation’s feasible spaces for the three-bus system. The feasible space for the OPF problem (5) is denoted by the red squares. The second-order mixed SDP relaxation gives the global optimum at the orange star. (b) shows that the second-order mixed SDP/SOCP relaxation is exact for the points near the specified scenario. However, this was not the case for all scenarios: (a) shows that the second-order mixed SDP/SOCP relaxation includes some points in the “hole” in the feasible space for which $\text{rank}(L_y\{\hat{x}\hat{x}^\top\}) > 1$. (a) Projection of the second-order mixed SDP/SOCP relaxation’s feasible space; (b) projection of the feasible space shown in (a) with $P_3 = 0$.

submatrices: the diagonal block corresponding to the degree-two monomials (i.e., $|\alpha| = 2$), which is identified by the green dashed highlighting in (14b), and the terms corresponding to the degree-zero, off-diagonal degree-two, and degree-four monomials (i.e., $|\alpha| = 2k$ for some $k \in \mathbb{N}$), which are identified by the blue dotted highlighting in (14b).

The first-order localizing “matrices” corresponding to the constraints (8b)–(8d) are, in fact, scalars.⁷ The corresponding scalar constraints in the first-order relaxation (13b)–(13g) are equivalent to the linear constraints in the SDP relaxation (8b)–(8d). The moment matrix in the first-order relaxation has all terms y_α such that $|\alpha| \leq 2$ (the diagonal block surrounded by the black line in (14b)), whereas the SDP relaxation has all terms y_α such that $|\alpha| = 2$ (the diagonal block with green dashed highlighting in (14b)). The degree-one terms (the terms with orange highlighting in (14b)) have odd $|\alpha|$ and so are unnecessary, as discussed earlier. Since the degree-one terms are unnecessary and $y_{00\dots 0} \geq 0$ by (13o), the positive semidefinite constraint on the first-order relaxation’s moment matrix (13n)

is equivalent to the positive semidefinite constraint in the SDP relaxation (8h). With an equivalent feasible space and objective function, the SDP relaxation in (8) is the same as the first-order ($\gamma = 1$) moment relaxation (13).

The moment matrix for the lower-order relaxation $\mathbf{M}_{\gamma-1}\{y\}$ is contained in the upper-left diagonal block of $\mathbf{M}_\gamma\{y\}$. Likewise, the upper-left diagonal block of the higher-order localizing matrices contain the lower-order localizing matrices. (The first-order matrices are contained within the solid black outlines in the second-order matrices in (14b) and (14c).) Since a necessary condition for a matrix to be positive semidefinite is positive semidefiniteness of all principal submatrices, the moment relaxations form a *hierarchy* where higher-order constraints imply the lower-order constraints.

Adding a rank-constraint $\text{rank}(L_y\{\hat{x}\hat{x}^\top\}) = 1$ to the SDP relaxation (8) yields a non-convex problem equivalent to the OPF problem (5). The SDP formulation (8) can thus be understood in terms of a rank relaxation. The higher-order moment relaxations generalize this approach by introducing constraints that are redundant in the OPF problem (5) but strengthen the moment relaxations. Consider $g(\hat{x})x_{\gamma-\eta}x_{\gamma-\eta}^\top \succcurlyeq 0$, where

⁷Observe that $L_y\{g(\hat{x})x_0x_0^\top\} = L_y\{g(\hat{x})\}$ since $x_0 = 1$.

$g(\hat{x}) \geq 0$ is a generic constraint in the OPF problem (5) with degree 2η . The rank-one matrix $x_{\gamma-\eta}x_{\gamma-\eta}^\top$ is positive semidefinite by construction, and the scalar constraint $g(\hat{x})$ is non-negative. Thus, their product is a rank-one positive semidefinite matrix. Relaxing to $L_y\{g(\hat{x})x_{\gamma-\eta}x_{\gamma-\eta}^\top\} \succeq 0$ (i.e., eliminating the rank constraint implied by $x_{\gamma-\eta}x_{\gamma-\eta}^\top$) results in the localizing matrix constraint.

The computational difficulty of solving the moment relaxations grows quickly with the relaxation order due to the size of the positive semidefinite matrix constraints. After elimination of V_{q1} using the angle reference constraint, the size of the moment matrix (13n) for the order- γ relaxation of a n -bus system is $(2n-1+\gamma)!/((2n-1)!\gamma!)$. For instance, the third-order relaxation of a 10 bus system has a matrix with size 1540×1540 . The “dense” formulation of the second-order relaxation is limited to solving problems with less than approximately ten buses [30]–[32]. By exploiting sparsity using techniques analogous to those for the SDP relaxation [47], the second-order relaxation is computationally tractable for systems with up to approximately 40 buses [33]. Extension to larger systems is possible by both exploiting sparsity and only applying the computationally intensive higher-order constraints to specific “problematic” buses [33], [34].

VI. MIXED SDP/SOCP RELAXATION HIERARCHY

The moment relaxations globally solve many OPF problems but are computationally challenging. First proposed in [39], a “mixed SDP/SOCP” hierarchy is tighter than the first-order moment relaxation but more tractable than the higher-order relaxations. This section describes this mixed SDP/SOCP hierarchy in the context of the example problem from Section IV.

The mixed SDP/SOCP hierarchy further relaxes the SDP constraints in the higher-order moment relaxations (13) to less stringent SOCP constraints. To ensure that the mixed SDP/SOCP relaxations are at least as tight as the first-order moment relaxation, positive semidefinite constraints are enforced for the diagonal block of the moment matrix that corresponds to degree-two monomials (i.e., y_α such that $|\alpha| = 2$, which are contained within the diagonal block highlighted in green dashed lines in (14b).) We relax the higher-order constraints using a necessary condition for a matrix to be positive semidefinite. Specifically, a necessary but not sufficient condition for a generic symmetric matrix \mathbf{W} to be positive semidefinite is given by the constraints:

$$\mathbf{W}_{ii} \geq 0 \quad i = 1, \dots, 2n \quad (15a)$$

$$\mathbf{W}_{ii}\mathbf{W}_{kk} \geq |\mathbf{W}_{ik}|^2 \quad \forall \{(i, k) \mid k > i\}. \quad (15b)$$

The mixed SDP/SOCP hierarchy enforces the higher-order constraints in the moment and localizing matrices using (15) for (13b)–(13g), (13j)–(13k), and (13n). Since the terms corresponding to odd-order monomials can be set to zero, this reduces to enforcing the SOCP constraints on the submatrices corresponding to those highlighted in blue in (14b) and (14c) for the three-bus system. For instance, in addition to non-negativity of the diagonal entries, the second-order mixed

SDP/SOCP hierarchy includes the following SOCP constraints associated with the moment matrix (14b):

$$\begin{aligned} y_{00}^{000}y_{00}^{400} &\geq |y_{00}^{200}|^2 \\ y_{00}^{000}y_{00}^{220} &\geq |y_{00}^{110}|^2 \\ &\vdots \\ y_{00}^{400}y_{00}^{220} &\geq |y_{00}^{310}|^2 \\ y_{00}^{400}y_{00}^{202} &\geq |y_{00}^{301}|^2 \\ &\vdots \\ y_{22}^{000}y_{04}^{000} &\geq |y_{13}^{000}|^2. \end{aligned}$$

Similarly, in addition a non-negative diagonal, the second-order mixed SDP/SOCP hierarchy enforces the following SOCP constraints associated with the localizing matrix (14c):

$$\begin{aligned} &\left((V_2^{\max})^2 y_{00}^{200} - y_{00}^{220} - y_{20}^{200} \right) \left((V_2^{\max})^2 y_{00}^{020} - y_{00}^{040} - y_{20}^{020} \right) \\ &\geq \left| (V_2^{\max})^2 y_{00}^{110} - y_{00}^{130} - y_{20}^{110} \right|^2 \\ &\left((V_2^{\max})^2 y_{00}^{200} - y_{00}^{220} - y_{20}^{200} \right) \left((V_2^{\max})^2 y_{00}^{002} - y_{00}^{022} - y_{20}^{002} \right) \\ &\geq \left| (V_2^{\max})^2 y_{00}^{101} - y_{00}^{121} - y_{20}^{101} \right|^2 \\ &\vdots \\ &\left((V_2^{\max})^2 y_{20}^{000} - y_{20}^{020} - y_{40}^{000} \right) \left((V_2^{\max})^2 y_{02}^{000} - y_{02}^{020} - y_{22}^{000} \right) \\ &\geq \left| (V_2^{\max})^2 y_{11}^{000} - y_{11}^{020} - y_{31}^{000} \right|^2. \end{aligned}$$

Since SOCP constraints have significant computational advantages over SDP constraints, the mixed SDP/SOCP relaxation is more tractable than the formulation of the moment relaxations given in Section V. Further, it is only necessary to enforce the SOCP constraints that correspond to higher-order polynomials which appear in a localizing matrix constraint. This provides additional computational advantages when combined with the approach of selectively applying the higher-order relaxation constraints [33]. See [39] for detailed numerical results demonstrating speed increases between a factor of 1.13 and 18.70 compared to the moment relaxations.

Fig. 7 shows the feasible space of active power injections for the second-order mixed SDP/SOCP relaxation. This figure was produced using the same gridding procedure employed in Fig. 6. The relaxation is exact for the specific loading condition $P_2 = P_3 = 0$ considered in Section IV and for nearby loading conditions (see the zoomed-in view of the feasible space shown in Fig. 7(b)). However, in contrast to the moment relaxations implemented with SDP constraints alone, illustrated in Fig. 6, the mixed SDP/SOCP relaxation was not exact for all scenarios. This is evident by the points that lie in the “hole” in the feasible space (i.e., the points in Fig. 7(a) that are not in Fig. 6(a)).⁸ As expected, mixed SDP/SOCP relaxations are generally not as tight as the moment relaxations in (13) which use only SDP constraints.

⁸The feasible spaces for the third- and fourth-order mixed SDP/SOCP relaxations also had points in this hole.

VII. CONCLUSION

An SDP relaxation globally solves many OPF problems which do not satisfy any existing sufficient conditions that assure exactness of the relaxation. This motivates the development of broader sufficient conditions, with a common conjecture being that some physical characteristics of the OPF problem can determine success or failure of the SDP relaxation. This paper has presented a small example OPF problem with two equivalent formulations. The SDP relaxation globally solves only one of the two formulations. This suggests that strictly physically based sufficient conditions for exactness of the SDP relaxation of the OPF problem cannot predict the relaxation's success or failure for all OPF problems.

The inability to develop universal, physically based sufficient conditions for success of the SDP relaxation motivates researching more sophisticated convex relaxations. We use the small example problem to illustrate two recently developed convex relaxation hierarchies: "moment" relaxations from the Lasserre hierarchy for polynomial optimization and a mixed SDP/SOCP hierarchy derived by relaxing the higher-order constraints in the moment relaxations. Both of these hierarchies generalize the SDP relaxation in order to enable global solution of a broader class of OPF problems.

REFERENCES

- [1] B. Lesieutre and I. Hiskens, "Convexity of the set of feasible injections and revenue adequacy in FTR markets," *IEEE Trans. Power Syst.*, vol. 20, no. 4, pp. 1790–1798, Nov. 2005.
- [2] W. Bukhsh, A. Grothey, K. McKinnon, and P. Trodden, "Local solutions of the optimal power flow problem," *IEEE Trans. Power Syst.*, vol. 28, no. 4, pp. 4780–4788, 2013.
- [3] M. Huneault and F. Galiana, "A survey of the optimal power flow literature," *IEEE Trans. Power Syst.*, vol. 6, no. 2, pp. 762–770, May 1991.
- [4] J. Momoh, R. Adapa, and M. El-Hawary, "A review of selected optimal power flow literature to 1993. Parts I and II," *IEEE Trans. Power Syst.*, vol. 14, no. 1, pp. 96–111, Feb. 1999.
- [5] Z. Qiu, G. Deconinck, and R. Belmans, "A literature survey of optimal power flow problems in the electricity market context," in *Proc. IEEE Power Syst. Conf. Expos. (PSCCE)*, Mar. 2009, pp. 1–6.
- [6] A. Castillo and R. O'Neill, "Survey of approaches to solving the ACOFP (OPF Paper 4)," U.S. Federal Energy Regulatory Commission Tech. Rep., Mar. 2013.
- [7] R. Zimmerman, C. Murillo-Sánchez, and R. Thomas, "MATPOWER: Steady-state operations, planning, and analysis tools for power systems research and education," *IEEE Trans. Power Syst.*, vol. 26, no. 1, pp. 12–19, 2011.
- [8] D. Molzahn, B. Lesieutre, and C. DeMarco, "A sufficient condition for global optimality of solutions to the optimal power flow problem," *IEEE Trans. Power Syst.*, vol. 29, no. 2, pp. 978–979, Mar. 2014.
- [9] S. Low, "Convex relaxation of optimal power flow: Parts I & II," *IEEE Trans. Control Network Syst.*, vol. 1, no. 1, pp. 15–27, Mar. 2014.
- [10] N. Shor, "Quadratic optimization problems," *Sov. J. Comput. Syst. Sci.*, vol. 25, pp. 1–11, 1987.
- [11] X. Bai, H. Wei, K. Fujisawa, and Y. Wang, "Semidefinite programming for optimal power flow problems," *Int. J. Electr. Power Energy Syst.*, vol. 30, no. 6/7, pp. 383–392, Jul.–Sep. 2008.
- [12] J. Lavaei and S. Low, "Zero duality gap in optimal power flow problem," *IEEE Trans. Power Syst.*, vol. 27, no. 1, pp. 92–107, Feb. 2012.
- [13] D. Molzahn, J. Holzer, B. Lesieutre, and C. DeMarco, "Implementation of a large-scale optimal power flow solver based on semidefinite programming," *IEEE Trans. Power Syst.*, vol. 28, no. 4, pp. 3987–3998, 2013.
- [14] E. Dall'Anese, H. Zhu, and G. Giannakis, "Distributed optimal power flow for smart microgrids," *IEEE Trans. Smart Grid*, vol. 4, no. 3, pp. 1464–1475, Sep. 2013.
- [15] M. Andersen, A. Hansson, and L. Vandenbergh, "Reduced-complexity semidefinite relaxations of optimal power flow problems," *IEEE Trans. Power Syst.*, vol. 29, no. 4, pp. 1855–1863, 2014.
- [16] L. Gan and S. Low, "Convex relaxations and linear approximation for optimal power flow in multiphase radial networks," in *Proc. 18th Power Syst. Comput. Conf. (PSCC)*, Aug. 18–22, 2014, pp. 1–9.
- [17] B. Kocuk, S. Dey, and A. Sun, "Strong SOCP relaxations of the optimal power flow problem," *Oper. Res.* [Online]. Available: <http://arxiv.org/abs/1504.06770>.
- [18] D. Bienstock and G. Munoz, "On linear relaxations of OPF problems," 2015, preprint. [Online]. Available: <http://arxiv.org/abs/1411.1120>.
- [19] C. Coffrin, H. L. Hijazi, and P. Van Hentenryck, "The QC Relaxation: A Theoretical and Computational Study on Optimal Power Flow," *IEEE Trans. Power Syst.*, vol. 31, no. 4, pp. 3008–3018, Jul. 2016.
- [20] E. Dall'Anese, S. Dhople, and G. Giannakis, "Regulation of dynamical systems to optimal solutions of semidefinite programs: Algorithms and applications to AC optimal power flow," in *Proc. Amer. Control Conf. (ACC)*, Jul. 1–3, 2015, pp. 2087–2092.
- [21] R. Madani, A. Kalbat, and J. Lavaei, "ADMM for sparse semidefinite programming with applications to optimal power flow problem," in *Proc. IEEE 54th Annu. Conf. Decision Control (CDC)*, Dec. 15–18, 2015, pp. 5932–5939.
- [22] C. Coffrin, H. Hijazi, and P. Van Hentenryck, "Strengthening convex relaxations with bound tightening for power network optimization," in *Principles and Practice of Constraint Programming*, ser. Lecture Notes in Computer Science, G. Pesant, Ed. Berlin/Heidelberg, Germany: Springer-Verlag, 2015, vol. 9255, pp. 39–57.
- [23] C. Coffrin, H. Hijazi, and P. Van Hentenryck, "Network flow and copper plate relaxations for AC transmission systems," 2015, preprint. [Online]. Available: <http://arxiv.org/abs/1506.05202>.
- [24] B. Kocuk, S. S. Dey, and X. A. Sun, "Inexactness of SDP relaxation and valid inequalities for optimal power flow," *IEEE Trans. Power Syst.*, vol. 31, no. 1, pp. 642–651, Jan. 2016.
- [25] C. Chen, A. Atamturk, and S. Oren, "Bound tightening for the alternating current optimal power flow problem," *IEEE Trans. Power Syst.*, to be published.
- [26] B. Lesieutre, D. Molzahn, A. Borden, and C. DeMarco, "Examining the limits of the application of semidefinite programming to power flow problems," in *Proc. 49th Annu. Allerton Conf. Commun., Control, Comput.*, Sep. 28–30, 2011, pp. 1492–1499.
- [27] D. Molzahn, B. Lesieutre, and C. DeMarco, "Investigation of non-zero duality gap solutions to a semidefinite relaxation of the power flow equations," in *Proc. 47th Hawaii Int. Conf. Syst. Sci. (HICSS)*, Jan. 6–9, 2014, pp. 2325–2334.
- [28] R. Madani, S. Sojoudi, and J. Lavaei, "Convex relaxation for optimal power flow problem: Mesh networks," *IEEE Trans. Power Syst.*, vol. 30, no. 1, pp. 199–211, Jan. 2015.
- [29] D. Molzahn, S. Baghsorkhi, and I. Hiskens, "Semidefinite relaxations of equivalent optimal power flow problems: An illustrative example," in *Proc. IEEE Int. Symp. Circuits Syst. (ISCAS)*, May 24–27, 2015, pp. 1887–1890.
- [30] D. Molzahn and I. Hiskens, "Moment-based relaxation of the optimal power flow problem," in *Proc. 18th Power Syst. Comput. Conf. (PSCC)*, Aug. 18–22, 2014, pp. 1–7.
- [31] C. Jozs, J. Maeght, P. Panciatici, and J. Gilbert, "Application of the moment-SOS approach to global optimization of the OPF problem," *IEEE Trans. Power Syst.*, vol. 30, no. 1, pp. 463–470, Jan. 2015.
- [32] B. Ghaddar, J. Marecek, and M. Mevissen, "Optimal power flow as a polynomial optimization problem," *IEEE Trans. Power Syst.*, vol. 31, no. 1, pp. 539–546, Jan. 2016.
- [33] D. Molzahn and I. Hiskens, "Sparsity-exploiting moment-based relaxations of the optimal power flow problem," *IEEE Trans. Power Syst.*, vol. 30, no. 6, pp. 3168–3180, Nov. 2015.
- [34] D. Molzahn, C. Jozs, I. Hiskens, and P. Panciatici, "Solution of optimal power flow problems using moment relaxations augmented with objective function penalization," in *Proc. IEEE 54th Annu. Conf. Decision Control (CDC)*, Dec. 15–18, 2015, pp. 31–38.
- [35] J.-B. Lasserre, *Moments, Positive Polynomials and Their Applications*. London, U.K.: Imperial College Press, 2010, vol. 1.
- [36] C. Jozs and D. Molzahn, "Moment/sums-of-squares hierarchy for complex polynomial optimization." [Online]. Available: <http://arxiv.org/abs/1508.02068>, 2015, submitted for publication.
- [37] J. Marecek and M. Takac, "A low-rank coordinate-descent algorithm for semidefinite programming relaxations of optimal power flow." [Online]. Available: <http://arxiv.org/abs/1506.08568>, preprint.
- [38] J. Liu, J. Marecek, and M. Takac, "Hybrid methods in solving alternating-current optimal power flows." [Online]. Available: <http://arxiv.org/abs/1510.02171>, preprint.

- [39] D. Molzahn and I. Hiskens, "Mixed SDP/SOCP moment relaxations of the optimal power flow problem," *Proc. IEEE Eindhoven PowerTech*, Jun. 2015.
- [40] R. Jabr, "Exploiting sparsity in SDP relaxations of the OPF problem," *IEEE Trans. Power Syst.*, vol. 27, no. 2, pp. 1138–1139, May 2012.
- [41] H. Willis, *Power Distribution Planning Reference Book*. New York, NY, USA: Marcel Dekker, 2004, pp. 1–6.
- [42] S. Deckmann, A. Pizzolante, A. Monticelli, B. Stott, and O. Alsac, "Studies on power system load flow equivalencing," *IEEE Trans. Power App. Syst.*, vol. PAS-99, no. 6, pp. 2301–2310, Nov. 1980.
- [43] S. Deckmann, A. Pizzolante, A. Monticelli, B. Stott, and O. Alsac, "Numerical testing of power system load flow equivalents," *IEEE Trans. Power App. Syst.*, vol. PAS-99, no. 6, pp. 2292–2300, Nov. 1980.
- [44] I. Hiskens and R. Davy, "Exploring the power flow solution space boundary," *IEEE Trans. Power Syst.*, vol. 16, no. 3, pp. 389–395, Aug. 2001.
- [45] F. Salam, L. Ni, S. Guo, and X. Sun, "Parallel processing for the load flow of power systems: The approach and applications," in *Proc. IEEE 28th Annu. Conf. Decision Control (CDC)*, Dec. 1989, pp. 2173–2178.
- [46] W. Bukhsh, A. Grothey, K. McKinnon, and P. Trodden, "Local solutions of optimal power flow," Univ. Edinburgh Sch. Math., Edinburgh Res. Group Optim., Edinburgh, U.K. Tech. Rep. ERGO-11-017, 2011.
- [47] H. Waki, S. Kim, M. Kojima, and M. Muramatsu, "Sums of squares and semidefinite program relaxations for polynomial optimization problems with structured sparsity," *SIAM J. Optim.*, vol. 17, no. 1, pp. 218–242, 2006.



Daniel K. Molzahn (S'09–M'13) received the B.S., M.S., and Ph.D. degrees in electrical engineering and the Masters of Public Affairs degree from the University of Wisconsin-Madison, WI, USA, where he was a National Science Foundation Graduate Research Fellow. He is a Computational Engineer at Argonne National Laboratory, Lemont, IL, USA. He recently completed the Dow Postdoctoral Fellow in Sustainability at the University of Michigan, Ann Arbor, MI, USA. His research focuses on power system optimization and control.



Ian A. Hiskens (F'06) is the Vennema Professor of Engineering with the Department of Electrical Engineering and Computer Science, University of Michigan, Ann Arbor, MI, USA. He has held prior appointments in the electricity supply industry (for ten years) and various universities in Australia and the United States. His research focuses on power system analysis, in particular the modelling, dynamics, and control of large-scale, networked, nonlinear systems. His recent activities include integration of renewable generation and new forms of load.

Prof. Hiskens is actively involved in various IEEE societies, and is VP-Finance of the IEEE System Council. He is a Fellow of Engineers Australia and a Chartered Professional Engineer in Australia.